Orbital Order and Possible Superconductivity in $LaNiO_3/LaMO_3$ Superlattices

Jiří Chaloupka[1,2] and Giniyat Khaliullin[1]

[1]*Max-Planck-Institut für Festkörperforschung, Heisenbergstrasse 1, D-70569 Stuttgart, Germany*
[2]*Institute of Condensed Matter Physics, Masaryk University, Kotlářská 2, 61137 Brno, Czech Republic*

(Received 3 July 2007; published 10 January 2008)

A hypothetical layered oxide La_2NiMO_6 where NiO_2 and MO_2 planes alternate along the c axis of ABO_3 perovskite lattice is considered theoretically. Here, M denotes a trivalent cation Al, Ga,... such that MO_2 planes are insulating and suppress the c-axis charge transfer. We predict that correlated e_g electrons in the NiO_2 planes develop a planar x^2-y^2 orbital order driven by the reduced dimensionality and further supported by epitaxial strain from the substrate. Low-energy electronic states can be mapped to a single-band $t - t' - J$ model, suggesting favorable conditions for high-T_c superconductivity.

DOI: 10.1103/PhysRevLett.100.016404 PACS numbers: 71.27.+a, 74.78.Fk, 75.30.Et

Despite decades of extensive research, cuprates remain the only compounds to date hosting the high-temperature superconductivity (SC). On empirical grounds, the key electronic and structural elements that support high T_c values are well known—no orbital degeneracy, spin one-half, quasi two-dimensionality (2D), and strong antiferromagnetic (AF) correlations. While these properties are partially realized in various materials (e.g., layered cobaltates), only cuprates possess all of them.

A unique feature of the high-T_c cuprates is the presence of an extended doping interval $0.05 \lesssim \delta \lesssim 0.20$ where the correlated electron maintains its (plane-wave–localized-particle) duality, and both fermionic and spin statistics may operate in physically relevant energy scales. The multifaceted behavior of electrons results in an exotic "normal" state of the cuprates with ill-defined quasiparticles, pseudogap, etc., which condenses into the superconducting state below T_c. There are a number of strongly correlated metallic oxides [1] based on $S = 1/2$ $3d$ ions as Ti^{3+} and V^{4+} (both with a single t_{2g} electron), Co^{4+} (a t_{2g} hole) and Ni^{3+} (closed t_{2g} shell plus one e_g electron) that possess a low-spin state in octahedral environment. These compounds show a great diversity of physical properties [1]; however, the mysterious strange-metal phase from which anomalous SC may emerge is missing.

Apart from dimensionality, the orbital degeneracy is "to blame" here. Originating from high symmetry of the MeO_6 octahedron—a common building block of both pseudocubic and layered perovskites,—the orbital degeneracy enlarges the Hilbert space and relaxes kinematical constraints on the electron motion. Consequently, a fermionic coherency is enhanced and doping induced insulator-metal transitions occur without a reference to the pseudogap phase. For example, in $La_{1-x}Sr_xTiO_3$ the formation of a three-band, correlated Fermi liquid completes within just a few percent doping range near $x \sim 0.05$ [2].

The orbital degeneracy strongly reduces AF correlations (believed to be crucial in cuprate physics), as electrons are allowed to have parallel spins residing on the different orbitals. This leads to competing Ferro- and AF-interactions that result in a rich variety of magnetic states in $S = 1/2$ oxides such as $RTiO_3$, Na_xCoO_2, Sr_2CoO_4, $RNiO_3$, $NaNiO_2$. In contrast, spin correlations in single-band cuprates are of AF nature exclusively and hence strong.

How to suppress the orbital degeneracy and promote cupratelike physics in other $S = 1/2$ oxides? In this Letter, we suggest and argue theoretically that this goal can be achieved in oxide superlattices. Specifically, we focus on Ni-based superlattices (see Fig. 1) which can be fabricated using recent advances in oxide heterostructure technology ([3–5] and references therein). While the proposed compound has a pseudocubic ABO_3 structure, its low-energy electronic states are confined to the NiO_2 planes and, hence, are of a quasi-2D nature. A substrate induced compression of the NiO_6 octahedra further stabilizes the x^2-y^2 orbital. Net effect is a strong enhancement of

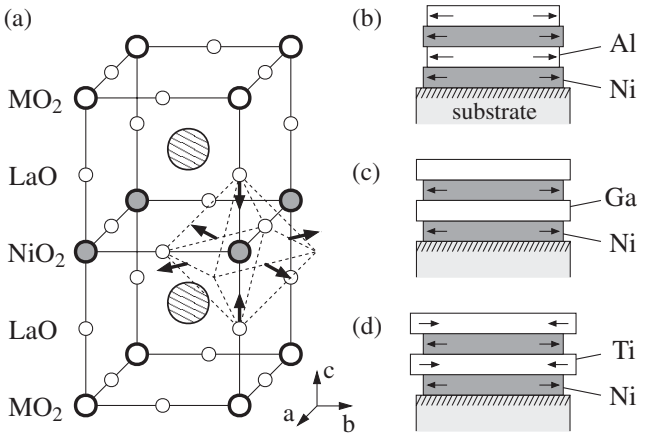

FIG. 1. (a) Superlattice La_2NiMO_6 with alternating NiO_2 and MO_2 planes. MO_2 layers suppress the c-axis hopping resulting in 2D electronic structure. Arrows indicate the c-axis compression of the NiO_6 octahedron imposed by tensile epitaxial strain and supported by Jahn-Teller coupling. (b) ,(c), (d) Strain-induced stretching of the NiO_2 planes occurs when superlattices with M = Al, Ga, Ti are grown on $SrTiO_3$ or $LaGaO_3$ substrates having large lattice parameter compared to that of $LaNiO_3$. Expected deformations are indicated by arrows.

AF correlations among spin one-half electrons residing predominantly on a single band of x^2-y^2 symmetry. Thus, all the "high-T_c conditions" are perfectly met. Moreover, the presence of a virtual $3z^2 - r^2$ orbital deforms the band dispersion compared to cuprates, leading to an enhanced next-neighbor hopping t' which is known to support higher T_c values [6].

The proposed superlattices can be viewed as a layer-by-layer "mixture" of a correlated e_g-band metal $LaNiO_3$ and a band insulator $LaMO_3$. The MO_2 planes with a trivalent M = Al or Ga serve here as block layers suppressing the c-axis hopping. The lattice parameters of $LaAlO_3$ ($\simeq$3.79 Å) and $LaGaO_3$ ($\simeq$3.89 Å) are close to that of $LaNiO_3$ ($\simeq$3.83 Å); further, NiO_2 and MO_2 planes have the same nominal charges. These factors should result in only a minimal structural and electronic mismatch, suggesting a stability of La_2NiMO_6 compounds. Yet another intriguing option is the case of M = Ti (the lattice parameter of $LaTiO_3$ is $\simeq$3.96 Å), where TiO_2 planes would themselves have a spin one-half residing on the t_{2g} orbital. As the t_{2g} shell of Ni^{3+} is full while the e_g level of Ti^{3+} is located well above the Fermi energy (roughly at $10Dq \sim$ 2 eV), the c-axis hoppings will be strongly suppressed again; therefore, NiO_2 and TiO_2 planes both develop quasi-2D electronic states of e_g and t_{2g} symmetry, respectively. While these states are not mixed by symmetry, the exchange of AF spin fluctuations will lead to a sizable interplane coupling, having interesting implications for magnetism and possible SC in La_2NiTiO_6.

The c-axis compression of the NiO_6 octahedra favoring x^2-y^2 orbital can be imposed by epitaxial strain from the substrate with a lattice parameter larger than that of $LaNiO_3$, e.g., on $LaGaO_3$ or $SrTiO_3$ ($\simeq$3.90 Å). The orbital selection by tuning epitaxial strain has been demonstrated in Ref. [3]; it is based on strong Jahn-Teller response of the e_g orbital on volume conserving distortions of the oxygen octahedron [7]. In superlattices of alternating NiO_2 and GaO_2 planes [Fig. 1(c)], strain effect should be more efficient as the lattice constants of $LaGaO_3$ and $SrTiO_3$ nearly match. Hence, lattice relaxation is reduced and thicker superlattices La_2NiGaO_6 can be grown. Further, using the $LaGaO_3$ substrate (instead of $SrTiO_3$) may help to disentangle the intrinsic physics within the *bulk* of La_2NiMO_6 superlattice from the charge-transfer effects at the *interface* between La_2NiMO_6 and the $SrTiO_3$ substrate, induced by different valences of Sr and La [4,8].

Now, we turn to the theoretical examination of our proposal. The formal valence state in the undoped case is Ni^{3+} in a low-spin configuration $t_{2g}^6 e_g^1$, and its fourfold degeneracy is specified by spin $S = 1/2$ and orbital pseudospin $\tau = \frac{1}{2}$. Because of strong pd covalency, wave functions are composed of the Ni e_g states and a proper combination of the oxygen p holes of the same e_g symmetry. In other words, the Ni^{3+} is shorthand notation for the $(NiO_{6/2})^{3-}$ complex with the same—spin doublet $\otimes$ orbital doublet—quantum numbers. Nearest-neighbor (NN) hopping matrix within the NiO_2 plane, as dictated by symmetry, is

$$t_{\alpha\beta} = \frac{t_0}{4}\begin{pmatrix} 3 & \mp\sqrt{3} \\ \mp\sqrt{3} & 1 \end{pmatrix}, \qquad \alpha, \beta \in \{x, z\}. \tag{1}$$

Here, $\{x \equiv x^2 - y^2, z \equiv 3z^2 - r^2\}$ basis is used, $\mp$ sign is valid for the a and b bond, respectively. We assume small c-axis hopping $\eta t_0 \ll t_0$ through the block MO_2 layers.

The tensile strain effect is modeled by orbital splitting $\Delta = \epsilon_z - \epsilon_x$. The (volume conserving) strain from $SrTiO_3$ substrate may provide $\sim$5% difference between the long or short axes of NiO_6 octahedron, nearly half of that in $LaMnO_3$ where this leads to 0.5–1.0 eV orbital splitting. Thus, $\Delta \sim$ 0.2–0.4 eV might be realistic.

The 3D nickelate $LaNiO_3$ is a correlated two-band metal. Nickelates of a smaller-radii rare-earth ions, where the bandwidth is reduced due to a stronger $GdFeO_3$-type distortion, undergo the insulating state at low temperature [9–12] and show a peculiar AF order [13]. Whether the 2D NiO_2 planes of La_2NiMO_6 are insulating or not has to be decided by experiment. Physically, the reduction of c-axis hopping and crystal-field splitting both should support the insulating state via the orbital disproportionation phenomenon in correlated systems [14]. In other words, correlations are effectively enhanced when the orbital degeneracy is lifted [15]. Based on these arguments, we consider below the insulating ground state.

We derived the superexchange Hamiltonian, including both intersite (dd) Ni^{3+}-$Ni^{3+} \rightarrow Ni^{4+}$-$Ni^{2+}$ and charge-transfer (CT) [16] Ni^{3+}-O^{2-}-$Ni^{3+} \rightarrow Ni^{2+}$-O-$Ni^{2+}$ processes, along the lines of Ref. [17]. The result for a bond $ij \parallel \gamma$ in the NiO_2 plane can be written as

$$H_{ij}^{(\gamma)} = J_0(K_{\sigma,\pm,\pm}^{dd} + K_{\sigma,\pm,\pm}^{\mathrm{CT}})\left(\tfrac{1}{2} \pm \hat{\tau}_i^{(\gamma)}\right)\left(\tfrac{1}{2} \pm \hat{\tau}_j^{(\gamma)}\right)\hat{P}_{\sigma,ij} \tag{2}$$

with an implied sum over $\sigma = 0, 1$ and all combinations of $\pm$, $\pm$. Here, $J_0 = 4t_0^2/U$, and U stands for the Coulomb repulsion on the same orbital. In the c axis, the CT part of (2) drops out and the rest is multiplied by small η^2. We have used projectors to a singlet and triplet state of two Ni^{3+} $S = 1/2$ spins: $P_{0,ij} = \frac{1}{4} - \boldsymbol{S}_i\boldsymbol{S}_j$ and $P_{1,ij} = \frac{3}{4} + \boldsymbol{S}_i\boldsymbol{S}_j$ respectively, and orbital projectors $\frac{1}{2} + \tau_i^{(\gamma)}$ and $\frac{1}{2} - \tau_i^{(\gamma)}$ selecting the planar orbital in the plane perpendicular to the γ axis and the directional orbital along this axis, e.g., $x^2 - y^2$ and $3z^2 - r^2$ orbitals, respectively, when $\gamma = c$. While the form (2) is determined by symmetry, the coefficients $K^{dd,\mathrm{CT}}$ are sensitive to the multiplet structure of excited states, as usual. Namely, they depend on two parameters J_H/U and $2U/(2\Delta_{\mathrm{pd}} + U_p)$ characterizing the strength of the Hund coupling and the strength of CT processes [16,17], respectively (explicit expressions will be given elsewhere [18]). In the following, we study the mean-field phase diagram depending on these two parameters.

The orbital state $|3z^2 - r^2\rangle \cos\frac{1}{2}\theta_i + |x^2 - y^2\rangle \sin\frac{1}{2}\theta_i$ is specified by the site-dependent orbital angle θ_i. We assume two sublattices with θ_A and θ_B in each NiO_2 plane and different spin arrangements and minimize superexchange $\langle H\rangle$ in this state. The result is the phase diagram in Fig. 2. The antiferromagnetic phase in the lower left part consists of pure x^2-y^2 planar orbitals (as in cuprates). At higher strengths of CT processes, this phase changes to the mixed orbital phases AAF, AAA, and AFA ($\theta_A = \theta_B$ evolve gradually from π to $\approx\pi/2$) with strongly anisotropic spin couplings. Upper in-plane ferromagnetic phases have staggered orbital order $\theta_A = 2\pi - \theta_B \approx \pi/2$.

The effect of the strain-induced field Δ on the phase diagram is dramatic. Even a very modest splitting Δ makes the planar-orbital phase a dominant one (Fig. 2).

Next, we address the effect of mobile holes (introduced either by an oxygen excess or by Sr doping). Evaluating (1) in our orbital state specified by $\{\theta_i\}$, we arrive at the effective NN hopping $\langle t_{\alpha\beta}\rangle_{ij} = t_0(2\cos\theta_- - \cos\theta_+ \mp \sqrt{3}\sin\theta_+)/4$, where $\theta_\pm = (\theta_i \pm \theta_j)/2$ (e.g., in the planar-orbital phase with $\theta = \pi$, one finds $\langle t\rangle = 3t_0/4$ as in cuprates). For a simple estimate, we add kinetic energy $-2|\langle t\rangle_a| - 2|\langle t\rangle_b|$ per hole to the superexchange energy. The modified phase diagram in Fig. 2 shows that the planar-orbital phase gains the largest kinetic energy and quickly spreads with δ.

The spin-exchange constant in the planar-orbital phase takes the familiar form (at $J_H/U = 0$) [16]: $J = (9t_0^2/4) \times [1/U + 2/(2\Delta_{\rm pd} + U_p)]$. With $t = 3t_0/4$ (hopping between the planar orbitals), the prefactor reads $4t^2$ as in cuprates. The value of J is not very sensitive to the strength of the Hund coupling; it is about 10% smaller at finite $J_H/U = 0.15$.

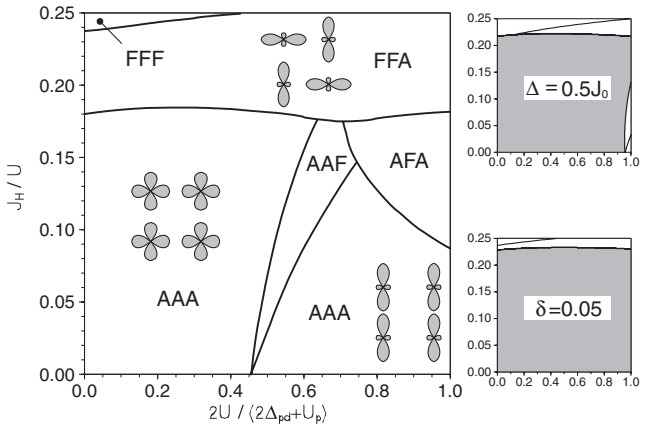

FIG. 2. Phase diagram of the spin-orbital Hamiltonian (2). The c-axis hopping is $0.3t_0$. The labels AAA, etc., indicate the magnetic order, with F (A) denoting parallel (antiparallel) orientations of the NN spins in the a, b, and c directions. Representative orbital states are sketched. In the pure planar-orbital phase (left-bottom), a weak A coupling between the layers is due to the higher order hoppings. Upper right panel: the phase diagram for $\Delta = \epsilon_z - \epsilon_x = 0.5J_0$, the gray area indicates the planar-orbital spin-AAA phase. Lower right panel: the phase diagram at 5% hole doping ($\Delta = 0$, $J = 0.3t_0$) shows that charge carriers strongly favor the planar-orbital phase.

At larger doping, the kinetic energy dominates and the spin order is lost. We show in the following that the orbital degeneracy is lifted again and the planar orbital is selected by correlated motion of holes. To address this regime, we adopt the multiorbital Gutzwiller approximation as described, e.g., in Ref. [19]. The hopping matrix elements are renormalized $t_{\alpha\beta} \to g_{\alpha\beta}t_{\alpha\beta}$ according to the orbital occupations via $g_{\alpha\beta} = 2\delta/\sqrt{(2 - n_\alpha)(2 - n_\beta)}$ (where $\alpha, \beta \in \{x, z\}$) and orbital splitting is adjusted $\Delta \to \tilde{\Delta}$ to minimize energy. The renormalized dispersion $\varepsilon_{\boldsymbol{k}}$ is then

$$\frac{2\varepsilon_{\boldsymbol{k}}}{t_0} = -g_+\gamma_+ \pm \sqrt{(g_-\gamma_+ + \tilde{\Delta}/t_0)^2 + 12g_{xz}^2\gamma_-^2} \quad (3)$$

apart from a $\boldsymbol{k}$-independent constant. Here $g_\pm = 3g_{xx} \pm g_{zz}$, and $\gamma_\pm = \frac{1}{2}(\cos k_a \pm \cos k_b)$.

Figure 3 shows bands $(\varepsilon_{\boldsymbol{k}} - \mu)/t_0$ and density of states for different dopings at bare orbital splitting $\Delta = 0.25t_0$. Correlations separate the bands and suppress the orbital mixing, such that the lower band is dominated by x^2-y^2 orbital and contains only a negligible $3z^2 - r^2$ fraction. A correlation-induced increase in orbital splitting [see Fig. 4(a)] and a reduced mobility of the $3z^2 - r^2$ orbital cooperate to lift the orbital degeneracy. The remaining effect of the initially degenerate $3z^2 - r^2$ orbital is a de-

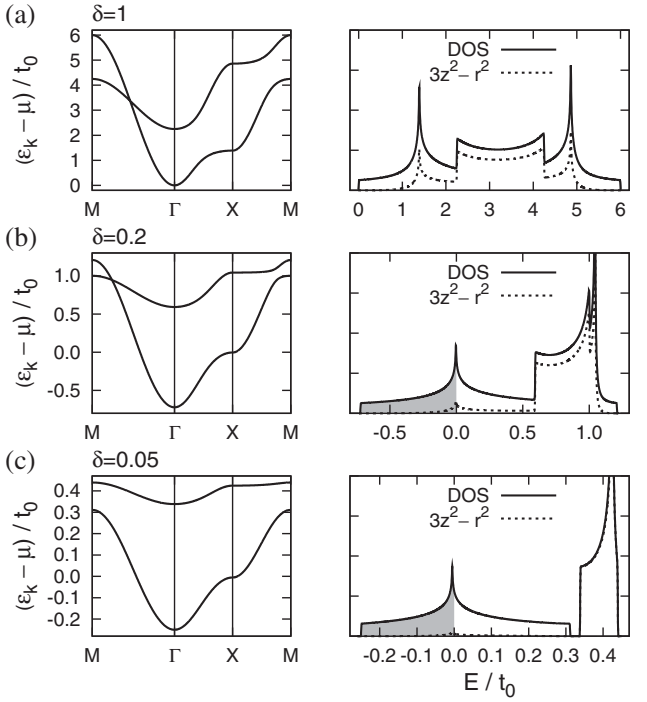

FIG. 3. The band structure and density of states for the e_g orbital splitting $\epsilon_z - \epsilon_x = 0.25t_0$ at doping levels (a) 100% (bare bands), (b) 20%, and (c) 5%. The dotted curves show the density of states projected onto the $3z^2 - r^2$ orbital. The gray areas indicate the occupied states at given δ.

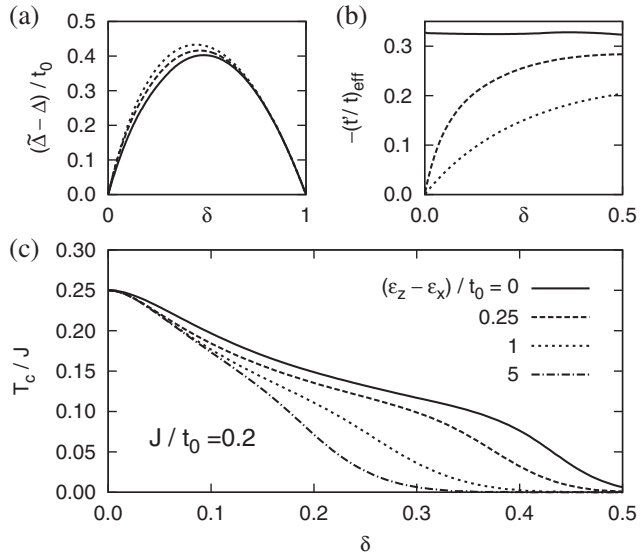

FIG. 4. (a) The correlation-induced correction to the orbital splitting, and (b) the effective t'/t as function of doping δ for different $\epsilon_z - \epsilon_x$. (c) The mean-field T_c [21] at various levels of e_g orbital splitting. The dashed-dotted line ($\epsilon_z - \epsilon_x = 5t_0$) corresponds to the "cuprate" situation with inactive $3z^2 - r^2$ state.

formation of the lower band of x^2-y^2 symmetry, so that the van Hove singularity stays close to the Fermi level.

The Fermi surface shape can exactly be reproduced by an effective $t - t'$ model with the dispersion relation $-2t(\cos k_a + \cos k_b) - 4t' \cos k_a \cos k_b$. The finite t'/t values [Fig. 4(b)] are generated solely by the presence of the second band, as we started with NN-only hopping.

Having a single band operating near the Fermi level, we may consider $t - t' - J$ model as in cuprates. To see effects of strain-induced splitting Δ (via ε_k) on possible SC, we estimated the T_c values within the mean-field treatment of $t - J$ model (see, e.g., Ref. [20]), i.e., from

$$1 = 2J \sum_k \frac{\gamma_-^2}{|\varepsilon_k - \mu|} \tanh \frac{|\varepsilon_k - \mu|}{2T_c}. \qquad (4)$$

We adopted here $J = 0.3t \approx 0.2t_0$ (a reasonable value for the planar orbitals), and ε_k is the lower branch of Eq. (3). The resulting T_c curves are shown in Fig. 4. As already observed in Fig. 3, the presence of virtual $3z^2 - r^2$ orbital deforms the band dispersion and enhances the density of states near the Fermi level. The corresponding T_c enhancement is clearly visible in Fig. 4.

Finally, superlattices with two subsequent NiO_2 planes, e.g. .../NiNi/Ga/NiNi/..., imitating double-layer cuprates should be interesting. As the planar-orbital ordering is quite robust, a breakdown of quasi 2D single-band picture is expected to occur at some larger critical number of the subsequent NiO_2 planes [22].

To conclude, we have pointed out that the orbitally nondegenerate spin one-half electronic structure—as in cuprates—is expected in the Ni-based superlattices. This suggests that artificially tailored superlattices may open new perspectives for the high-T_c superconductivity. We hope that the theoretical expectations for our particular proposal—"the double perovskite" La_2NiMO_6—are encouraging enough to motivate experimental efforts.

We would like to thank B. Keimer, J. Chakhalian, O. K. Andersen, and P. Horsch for stimulating discussions.

[1] M. Imada, A. Fujimori, and Y. Tokura, Rev. Mod. Phys. **70**, 1039 (1998).
[2] Y. Tokura *et al.*, Phys. Rev. Lett. **70**, 2126 (1993).
[3] M. Izumi *et al.*, Mater. Sci. Eng. B **84**, 53 (2001).
[4] A. Ohtomo, D. A. Muller, J. L. Grazul, and H. Y. Hwang, Nature (London) **419**, 378 (2002).
[5] J. Chakhalian *et al.*, Nature Phys. **2**, 244 (2006).
[6] E. Pavarini *et al.*, Phys. Rev. Lett. **87**, 047003 (2001).
[7] T. Kimura and Y. Tokura, Annu. Rev. Mater. Sci. **30**, 451 (2000).
[8] S. Okamoto and A. J. Millis, Nature (London) **428**, 630 (2004).
[9] J. B. Torrance *et al.*, Phys. Rev. B **45**, 8209 (1992).
[10] J. A. Alonso *et al.*, Phys. Rev. Lett. **82**, 3871 (1999).
[11] J.-S. Zhou and J. B. Goodenough, Phys. Rev. B **69**, 153105 (2004).
[12] J.-S. Zhou, J. B. Goodenough, and B. Dabrowski, Phys. Rev. Lett. **95**, 127204 (2005).
[13] V. Scagnoli *et al.*, Phys. Rev. B **73**, 100409(R) (2006).
[14] N. Manini, G. E. Santoro, A. Dal Corso, and E. Tosatti, Phys. Rev. B **66**, 115107 (2002).
[15] O. Gunnarsson, E. Koch, and R. M. Martin, Phys. Rev. B **54**, R11026 (1996).
[16] M. V. Mostovoy and D. I. Khomskii, Phys. Rev. Lett. **92**, 167201 (2004).
[17] A. M. Oleś, G. Khaliullin, P. Horsch, and L. F. Feiner, Phys. Rev. B **72**, 214431 (2005).
[18] J. Chaloupka and G. Khaliullin (unpublished).
[19] S. Zhou *et al.*, Phys. Rev. Lett. **94**, 206401 (2005).
[20] F. C. Zhang, C. Gros, T. M. Rice, and H. Shiba, Supercond. Sci. Technol. **1**, 36 (1988).
[21] To be understood as a "pseudogap temperature" at small doping δ. To estimate the true SC temperature one has to multiply the T_c curves by $g \approx 2\delta$ [20].
[22] At a first glance, La_2NiMO_6 superlattice might seem as an analog of layered perovskite $La_{2-x}Sr_xNiO_4$ at $x \simeq 1$ compositions [R. J. Cava *et al.*, Phys. Rev. B **43**, 1229 (1991)], where *an average* valence state is Ni^{3+}. However, there are two crucial differences. First, $LaSrNiO_4$ is a *solid solution* of La and Sr where large local variations of the ratio La/Sr (forming perhaps some patterns) are possible. This should lead to mixed valence states $Ni^{2+,3+,4+}$ and strong disorder effects. Second, there is no compression of NiO_6 octahedra in $La_{2-x}Sr_xNiO_4$, which are rather elongated at small x and become of a regular shape at $x \simeq 1$. For these reasons, La_2NiMO_6 superlattice and $La_{2-x}Sr_xNiO_4$ solid solution should have different properties.